Int. J. Engng Ed. Vol. 25, No. 6, pp. 1077–1091, 2009
Printed in Great Britain.

0949-149X/91 $3.00+0.00

Getting Smarter about Accuracy Tuning Multi-Physics Simulations*

A. J. BAKER, S. SAHU, M. A. GRUBERT AND S. C. ERICSON
Computational Fluid Dynamics Laboratory, University of Tennessee, Knoxville, TN 37966-2030, USA.
E-mail: ajbaker@utk.edu Sahu_Sunil@cat.com marcel.a.grubert@exxonmobil.com sce@cfdrc.com

Finite element analysis (FEA) has totally penetrated industry in support of engineered systems design optimization. Over its half century of development, numerous commercial FEA codes have been created to support the distinct engineering disciplines constituting continuum mechanics. Conversely, modern engineering systems design spans multi-disciplines requiring multi-physics analyses of the type supported by COMSOL. As many practicing computational design engineers matriculate without formal academic exposure to the theoretical underpinnings of FEA, familiarity with quantitative assessment protocols for estimating engineering accuracy of multi-physics predictions is weak. The solution to this technical base shortfall is detailed.

Keywords: finite element analysis; problem solving environment; error estimation theory; solution adaptive mesh refinement; engineering accuracy

INTRODUCTION

THE ABILITY TO ROUTINELY PERFORM multi-physics simulations of engineered systems presents an exciting opportunity to optimize design, provided the generated data indeed meet the criterion of engineering accuracy. Real world applications invariably couple conservation principles across the spectrum of engineering continuum mechanics disciplines including structural mechanics, vibrations, fluid dynamics, heat/mass transport, acoustics, electromagnetics, etc. The resultant academic discipline becoming a standard component of undergraduate (UG) engineering education is the computational engineering sciences, which starting with the fundamental mechanics conservation principles of mass, momentum, energy, etc., converts these partial differential equation systems (PDEs) into computable form in the modern context of weak form theory.

The progenitor of weak form theory for the computational engineering sciences is the finite element method, developed and put into practice in the late 1950s by aeronautical engineers to analyze aircraft structural components. Exploratory musings preceded this step, e.g. Hrenikoff [1] who in 1941 developed an elasticity solution for torsion problems based on triangles, and in 1943 Courant [2] published a variational formulation for problems in vibrations. Turner, et al [3] were the first to derive the stiffness matrix for truss and beam analysis, and Clough [4] first coined the term finite element in 1960. Shortly thereafter, Argyris [5] published the first monograph detailing a formal mathematical foundation for the engineers' emergent finite element analysis (FEA).

The pioneering application of FEA to the nonstructural problem of unsteady heat transfer was based on the variational calculus, Zienkiewicz and Cheung [6]. As the variational underpinnings matured, the mechanistic engineering concepts supporting FEA became replaced by classical Rayleigh-Ritz methodology, Rayleigh [7], Ritz [8]. At the same time, chemical engineers were using algorithms based on the method of weighted residuals (MWR), with Finlayson [9] publishing the pioneering 1972 exposition. In MWR, the discrete approximation error was constrained by requiring local integrals containing select "weights" to vanish. Within the class, collocation was recovered for Dirac delta weights, a finite volume algorithm was retrieved for a constant weight, least squares resulted for weights of the PDE operator itself, and selecting weights identical to the discrete trial functions reproduced the Galerkin criteria, named after the 1915 (non-discrete) theory of B.G. Galerkin [10].

MWR constructions removed the linearity constraint of Rayleigh-Ritz theory via the Green-Gauss form of the Divergence Theorem of calculus. This discovery enabled derivation of FEA methods for explicitly nonlinear problems, specifically computational fluid dynamics (CFD), with 1970s pioneering contributions from Oden [11, 12], Baker [13, 14], Olson [15], and Lynn [16]. The evolution of modern approximation theory occurred coincidentally, Oden and Reddy [17], leading to research focused on validating theoretical asymptotic error estimates for nonlinear CFD problem statements, Popinski and Baker [18], Soliman and Baker [19, 20]. The first text was *Finite Element Techniques for Fluid Flow*, published by

* Accepted 12 August 2009.

Connor and Brebbia [21] in 1974. There shortly followed *Finite Element Simulation in Surface and Subsurface Hydrology*, Pinder and Gray [22], and *Finite Element Computational Fluid Mechanics*, Baker [23].

The modern approximation theory foundation for quantifying FEA performance is fully matured, c.f. Oden and Demkowicz [24], but has yet to penetrate the professional simulation workplace. Since FEA underlies any multi-physics problem solving environment (PSE), specifically COMSOL, it is imperative that such code users gain expertise in assessment protocols to ensure an FEA solution exhibits engineering accuracy and is the best achievable (optimal) in terms of computer resource expenditure. In reality, a multi-physics simulation is an experiment executed in the computational laboratory. Rather than scale modeling, as done in the traditional engineering laboratory, a multi-physics simulation requires approximating the mathematical description solution, the heart of FEA. One must further identify appropriate boundary conditions (BCs), and perhaps an initial condition (IC), while the physics closure model involves typically force-flux assumptions with material dependent properties, e.g. viscosity, conductivity, permittivity, emissivity, or solution dependent models, e.g. visco-plasticity, turbulent heat/mass transport, . . .

Completing the analogy, one measures data in the legacy laboratory, then interpolates to isolate data points exhibiting error followed by results interpretation to determine engineering usefulness. In the multi-physics computational laboratory, the FEA solution data embed the consequence of all approximations underlying the defined mathematics-physics-discretized process. These data must correspondingly be analyzed for error to quantitatively validate engineering accuracy, hence usefulness in the support of design optimization.

MULTI-PHYSICS SIMULATION ERROR MECHANISMS

The goal of any computational experiment is to generate a quality approximate solution to a PDEs + BCs + IC problem statement in engineering continuum mechanics, as closed by defining physics closure relations for viscosity, thermal conductivity, mass diffusivity, permittivity, eddy viscosity, etc. Let $\mathcal{L}(q(\mathbf{x},t)) = 0$ denote a multi-physics PDE statement, the exact solution $q(\mathbf{x},t)$ to which of course is unknown! Denoting any approximate solution as $q^N(\mathbf{x},t)$, the resultant approximation error $e^N(\mathbf{x},t)$ is

$$e^N(\mathbf{x},t) \equiv q(\mathbf{x},t) - q^N(\mathbf{x},t) \qquad (1)$$

a distributed function of space and time on the problem statement domain of dependence.

The modern underpinnings of FEA theory assert that any approximate solution, also a continuum distributed function of space and time, can be expressed as

$$q^N(\mathbf{x},t) \equiv \sum_{\alpha=1}^{N} \Psi_\alpha(\mathbf{x}) Q_\alpha(t) \qquad (2)$$

In (2), the trial space $\Psi_\alpha(\mathbf{x})$ is a set of functions having assumed known spatial dependence, while $Q_\alpha(t)$ is the set of *unknown* perhaps time-dependent expansion coefficients. These are called degrees-of-freedom (DOF) in an FEA implementation, and it is their determination that produces the sought solution $q^N(\mathbf{x},t)$.

The obvious goal of FEA theory is to extremize the error (1), i.e., render it as small as possible! For the distributions $q^N(\mathbf{x},t)$ and $e^N(\mathbf{x},t)$, the precise recipe formulated by the mathematics community is to determine the extremum (stationary point) of a weak form, an integral containing *all* arbitrary test functions. The optimal choice for the test function set is identically the trial space $\Psi_\alpha(\mathbf{x})$, and the resultant weak form extremum is the Galerkin weak statement (GWS^N)

$$\mathrm{GWS}^N \equiv \int_\Omega \Psi_\beta(\mathbf{x}) \mathcal{L}(q^N(\mathbf{x},t)) \mathrm{d}\tau \equiv \{0\}, \quad \textit{for } 1 \le \beta \le N \qquad (3)$$

In the continuum, (3) states that the approximation error $e^N(\mathbf{x},t)$ is rendered *orthogonal* (mathematically perpendicular) to every member of the trial space $\Psi_\alpha(\mathbf{x})$ over the entire n-dimensional spatial span of the problem statement solution domain Ω. The weak statement (3) generates *exactly* N equations, typically written as a matrix statement. Following BCs imposition, the matrix order N is appropriately reduced to the rank precisely equal to the DOF requiring determination, as defined in the approximate solution (2).

The error mechanisms intrinsic to the process (1)–(3) can be independently categorized as: approximation error, dispersion error, numerical diffusion error and input data error. The available theoretical analyses quantifying each error type, hence assessment protocols as a function of characterizing non-dimensional (non-D) groups, e.g., Reynolds, Prandtl, Nusselt, Schmidt, Debye numbers (Re, Pr, Nu, Sc, De, etc), is now detailed.

Approximation error

The GWS^N theory (1)–(3) is elegantly simple but how does one identify a suitable trial space $\Psi_\alpha(\mathbf{x})$, hence evaluate the associated N integrals defining the extremum? The FEA response is to discretize the PDE solution domain Ω into many small non-overlapping cells, called finite elements Ω_e, which geometrically appear as line segments, triangles, tetrahedra, hexahedra, etc, c.f., Baker [25, Ch. 5]. For each such geometric entity Ω_e define the trial space basis function $\{N_k(\mathbf{x})\}$, a column matrix containing pertinent members of $\Psi_\alpha(\mathbf{x})$ typically

selected as interpolation polynomials of completeness degree k. Each $\{N_k(\mathbf{x})\}$ spans *only* a single Ω_e, a much less challenging task than identifying the members of $\Psi_\alpha(\mathbf{x})$ which span the global spatial domain Ω!

For superscript h denoting spatial discretization, the continuum statement of error and solution approximation (1)–(2) is altered to

$$q^N(\mathbf{x},t) \equiv \sum_{\alpha=1}^{N} \Psi_\alpha(\mathbf{x}) Q_\alpha(t) \Rightarrow q^h(\mathbf{x},t) \equiv q(\mathbf{x},t) - e^h(\mathbf{x},t) \quad (4)$$

where $e^h(\mathbf{x},t)$ is the resultant FE solution approximation error. The precise statement of the FE discrete approximate solution is

$$q^h(\mathbf{x},t) \equiv \cup_e^M q_e(\mathbf{x},t), \quad q_e(\mathbf{x},t) \equiv \{N_k(\mathbf{x})\}^T \{Q(t)\}_e \quad (5)$$

where $\{Q(t)\}_e$ contains those $Q_\alpha(t)$ in (2) associated only with Ω_e, and $\cup_e^{\mathrm{M}}$ denotes union (non-overlapping sum) over the M domains Ω_e constituting the mesh Ω^h. The resultant FE discretely implemented Galerkin weak statement replacement for (3) is

$$\mathrm{GWS}^h \equiv \cup_e^{\mathrm{M}} \int_{\Omega_e} \{N_k(\mathbf{x})\} \mathcal{L}(q_e(\mathbf{x},t)) \mathrm{d}\tau \equiv \{0\}, \quad \textit{for } 1 \le e \le M \quad (6)$$

With (4)–(6), a PSE such as COMSOL readily computes the integrals defined in GWS^h, then solves the resultant algebraic matrix statement for the DOF associated with the coefficient set $Q_\alpha(t)$. Since the FE process is founded on interpolation polynomials, the available theory naturally bounds the discrete approximation error $e^h(\mathbf{x},t)$ by interpolation error. The proof, [17, Ch. 8], states that under *solution adapted regular mesh refinement*, and for Pa the placeholder for the pertinent non-D group (Re, Pr, etc), the FE discrete solution approximation error $e^h(\mathbf{x},n\Delta t)$ at solution time $n\Delta t$ asymptotically vanishes as

$$\textit{for } \mathrm{Pa}^{-1} > 0 : \left\|e^h(n\Delta t)\right\|_E \le \mathrm{C}h^{2\gamma} \left(\|\mathrm{data}\|^2_{\mathrm{L2},\Omega} + \|\mathrm{data}\|^2_{\mathrm{L2},\Omega}\right) + \mathrm{C}_t \Delta t^{f(\theta)} \|q_0\|_E \quad (7)$$

$$\gamma = \min(k+m-1, r-m)$$

$$\textit{for } \mathrm{Pa}^{-1} = 0 : \left\|e^h(n\Delta t)\right\|_E \le \mathrm{C}h^2 \int_{t_0}^{n\Delta t} \|q(\mathbf{x},\tau)\|^2_{\mathrm{H}^{k+1}} \mathrm{d}\tau + \mathrm{C}_t \Delta t^{f(\theta)} \|q_0\|_E \quad (8)$$

The caveats and definitions pertinent to (7)–(8) are:

- solution adapted: use finer meshings where larger solution gradients exist
- regular refinement: maintain Ω_e geometric aspect ratios during mesh refinement
- $\left\|e^h(n\Delta t)\right\|_E$: the energy norm (an integral) of the error existing at elapsed time $n\Delta t$ into the solution $q^h(\mathbf{x},t)$ evolution
- h : the measure (a length scale) of the characteristic Ω_e of the mesh Ω^h
- γ : the exponential rate of error decrease under mesh refinement, where
  k = FE basis $\{N_k(\mathbf{x})\}$ completeness degree
  m = (1,2) for laplacian, biharmonic PDE operators
  r = a measure of data non-smoothness, rough data degrades convergence
- $\|\mathrm{data}\|^2_{L2,\Omega,\partial\Omega}$: the L2 (mean square) norm measuring the *size* of given information (data) driving $q^h(\mathbf{x},t)$ evolution, in the domain Ω and on the boundary $\partial\Omega$
- $\|q_0\|_E$: the interpolation of the problem IC onto the nodes of the mesh Ω^h
- C, C_t: theory constants, always unknown (but never required!)
- $\Delta t^{f(\theta)}$: time integration step size, raised to the truncation error order of the selected algorithm parameterized by an implicitness factor θ
- $\int_{t_0}^{n\Delta t} \|q(\mathbf{x},\tau)\|^2_{\mathrm{H}^{k+1}} \mathrm{d}\tau$: the integral of exact solution evolution to elapsed time $n\Delta t$, the *data* multiplier for a hyperbolic PDE, which predicts convergence is independent of basis completeness degree k.

Should the subject PDEs + BCs statement be independent of time, (7)-(8) remain pertinent upon deleting $(n\Delta t)$ in the norm argument and setting $\mathrm{C}_t = 0$.

So how does one use (7)–(8) to generate a quantitative measure of the accuracy of the FE solution $q^h(\mathbf{x},t)$? The answer is to execute a solution adapted regular mesh refinement study guided by the fundamental FE solution statement (4). This operation generates data amenable to evaluating the sequence of refined mesh FE solution norms

$$\left\|q^h\right\|_E + \left\|e^h\right\|_E = \|q\|_E = \left\|q^{h/2}\right\|_E + \left\|e^{h/2}\right\|_E = \left\|q^{h/4}\right\|_E + \left\|e^{h/4}\right\|_E + \ldots = \left\|q^{h/\mathrm{n}}\right\|_E + \left\|e^{h/\mathrm{n}}\right\|_E \quad (9)$$

which upon substitution of definition (7) or (8) for each mesh Ω^h, $\Omega^{h/2}$, $\Omega^{h/4}$, . . ., $\Omega^{h/\mathrm{n}}$, eliminates all embedded unknown constants and the unknown data norms $\|\mathrm{data}\|^2_{L2,\Omega,\partial\Omega}$. The resultant precise quantitative statement for the discrete approximation error measure for the finest mesh $\Omega^{h/\mathrm{n}}$ solution is

$$\left\|e^{h/\mathrm{n}}(n\Delta t)\right\|_E = \frac{\Delta\left\|q^{h/\mathrm{n}}\right\|_E}{2^{2k}-1}, \quad \textit{where } \Delta\left\|q^{h/\mathrm{n}}\right\|_E \equiv \left\|q^{h/\mathrm{n}}(n\Delta t)\right\|_E - \left\|q^{h/\mathrm{n}-1}(n\Delta t)\right\|_E \quad (10)$$

The norms defining the sequence $\Delta\left\|q^{h/\mathrm{n}}\right\|_E$, etc., are readily evaluated using the generated FE

discrete solutions. The energy norm definition is intrinsically tied to the given PDEs + BCs + IC statement. For exposition, the PDE + BCs system for convective energy transport is

$$\mathcal{L}(T) = \frac{\partial T}{\partial t} + u \cdot \nabla T - \frac{1}{\mathrm{Re\,Pr}} \nabla \cdot \kappa \nabla T - s = 0\,, \quad on\ \Omega \times t \tag{11}$$

and the general BC statement is of the Robin type

$$\ell(T) = \hat{\mathbf{n}} \cdot \nabla T \ + \mathrm{Nu}(T - T_r) = 0, \ \ on\ \partial\Omega \times t \tag{12}$$

where Re, Pr and Nu are the Reynolds, Prandtl and Nusselt numbers, respectively. Thereby, in (7)–(8) Pa = RePr, a typically quite large number. Further, $\kappa(T)$ is the non-D temperature-dependent thermal diffusivity distribution and T_r is the convective exchange temperature.

The energy norm definition for (11)–(12) is

$$\| T(t)\|_E \ \equiv \frac{1}{2\mathrm{Re\,Pr}} \int_\Omega [\kappa \nabla T \cdot \nabla T]\, d\tau + \frac{\mathrm{Nu}}{2\mathrm{Re\,Pr}} \int_{\partial\Omega_n} \left[\kappa(T)^2\right] d\sigma \tag{13}$$

which is indeed a scalar at time t, i.e. a number, once $T(\mathbf{x}, t)$ is known. The norm for the discrete FE solution $T^h(\mathbf{x}, n\Delta t)$ involves substitution of (5) into (13) yielding summation of the resultant integrals over $\Omega^{h/\mathrm{n}} = \cup_e^{\mathrm{M}} \Omega_e$ of the FE element-level expression

$$\left\| T^h(\Omega_e, n\Delta t)\right\|_E \equiv \frac{1}{2\mathrm{Re\,Pr}} \left[\int_{\Omega_e} [\kappa \nabla T_e \cdot \nabla T_e]\, d\tau + \ \mathrm{Nu} \int_{\partial\Omega_e \cap \partial\Omega_n} \left[\kappa(T_e)^2\right] d\sigma \right] \tag{14}$$

This generates the distribution of scalars $\left\|e^h(\Omega_e, n\Delta t)\right\|_E$, and the available theory for solution adapted regular mesh refinement confirms the optimal solution for any mesh M is that which equi-distributes the solution energy (norm) (14), Babuska and Rheinboldt, [26]. Thereby, searching the array $\left\|e^h(\Omega_e, n\Delta t)\right\|_E$ for local extrema provides precise guidance on solution adapting the regular mesh refinement process. Its completion generates data confirming the asymptotic convergence rate of the FE discrete solution, including those for explicitly nonlinear PDEs + BCs + IC statements, is indeed accurately characterized by (7) or (8).

Dispersion error

Equations (7)–(8) clearly confirm that GWS^h solution accuracy is mesh density dependent, which introduces the issue of solution *spectral content resolution* on a mesh Ω^h of measure h (distribution). The COMSOL solution process generates the DOF set for (5) located at least at each geometric singularity (vertex node) of the Ω_e constituting Ω^h, illustrated in the left graphic of Figure 1. Spectral resolution is easily visualized via a Fourier representation, and drawing a single sine wave through 3 adjacent nodes, middle graphic, generates vertex DOF that are zero! Clearly then, spectral content of wavelength $2h$ cannot be resolved at all on a mesh of measure h! Conversely, spectral wavelength content spanning several h, right graphic, is readily resolved via the FE trial space basis solution DOF $Q_\alpha(n\Delta t)$.

For PDEs possessing nominal Pa^{-1} and devoid of first spatial derivatives, FE solution asymptotic convergence theory suffices as spectral content resolution is not an issue unless the defining data are non-smooth, i.e. the r term in the definition of γ, (7)–(8), dominates. Conversely, for PDEs with relatively small Pa^{-1} and/or containing first derivatives, e.g., (11), the fidelity of (7)–(8) in error characterization can be overwhelmed by dispersion error, the cascading of the unresolved $2h$ spectral content into longer wavelength solution oscillations spanning scale multiples of h.

The theoretical analysis characterizes algorithm discrete solution dispersion error propagation via Taylor series in Fourier space spanned by non-D wavenumber $m = \kappa/h$, [27]. For the limiting case $\mathrm{Pa}^{-1} = 0$, Figure 2 graphs the theory prediction comparing select finite difference (labeled FD, UW), finite volume (Q3, Q5) and FE (GL, GQ, GC) algorithms as percent error in exact propagation of a single Fourier mode, labeled phase velocity error, versus integer multiples of the mesh measure with h replaced by Δx. The abscissa is scaled logarithmically to expand the all important short wavelength, i.e., large wavenumber, region. Note that *all* algorithms tested possess 100% phase velocity error at wavelength $2h$ =

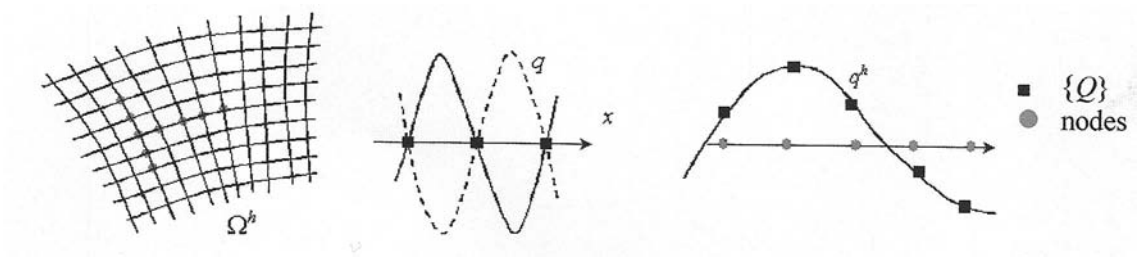

Fig. 1. Domain discretization, resolution on a mesh of measure h, from [25].

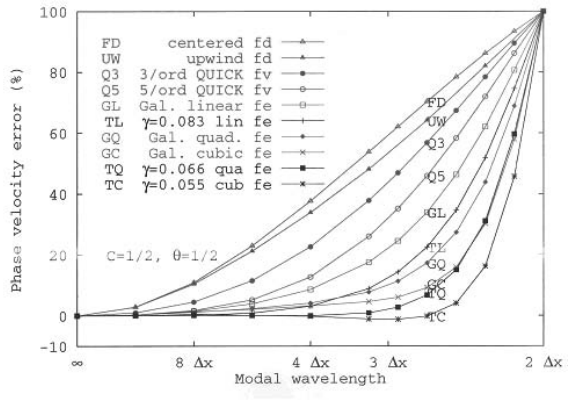

Fig. 2. Fourier spectral theory prediction of algorithm phase velocity error distributions, from [28].

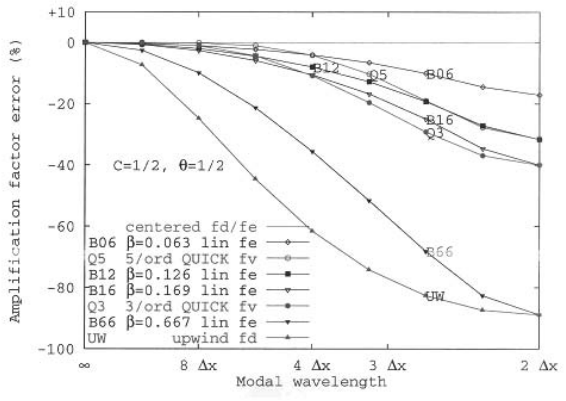

Fig. 3. Fourier spectral theory prediction of algorithm amplification factor error distributions, from [28].

$2\Delta x$ confirming the middle graphic in Figure 1. The theory predicts that Galerkin FE algorithms are superior to the alternative theory constructions, and that GWS^h algorithms implemented using FE linear, quadratic and cubic completeness degree bases $\{N_k(\mathbf{x})\}$, $1 \leq k \leq 3$ in (5), exhibit progressively superior error diminution. Finally, the accuracy performance of each GWS^h algorithm can be improved via a Taylor series manipulation (labeled TL, TQ, TC), [28].

Numerical diffusion error

Discrete approximation dispersion error generates mesh scale oscillations which, in the presence of non-linearities intrinsic to multi-physics statements, especially CFD, destabilizes the matrix algebra iteration process of the PSE. The universally used containment mechanism is to embed numerical diffusion to artificially dissipate such mesh scale oscillations, hence regain algebraic stability. The numerous forms of these input mechanisms are Taylor series truncation error categorized as (order) $O(h^p)$ additions, with $1 \leq p < 3$ typical in commercial code practice. The lowest order $p = 1$ method, called upwind (UW), generates artificial physics that can totally overwhelm the action of the genuine physics characterized by Pa^{-1}. Code tutorials specify transition from $p = 1$ to a $p \geq 2$ method, following startup from a (usually poor) IC, which better matches the Taylor series order of the underlying discrete numerics. Fortunately, numerical diffusion error can asymptote to zero faster than the discrete approximation error (5), hence properly performed solution adapted regular mesh refinement is the key to control of this error mechanism as well.

Wavenumber space Fourier spectral analysis theory also fully characterizes numerical diffusion operator effects. For the range of discrete algorithms compared in Figure 2, the companion theory prediction of propagated signal magnitude loss is labeled amplification factor *error* in Figure 3 as a function of modal wavelength. Standard finite difference and all GWS^h algorithms (labeled centered (fd/fe) inject no artificial diffusion. The upwind finite difference (UW) and both finite volume (Q3, Q5) algorithms possess the graphed error distributions, with extremum at the unresolved wavelength 2Δx. The Taylor series modified $k = 1$ basis GWS^h algorithm generates numerical diffusion spectra with magnitude controlled by an added β-term nonlinear operator, labeled B66 $\rightarrow$ B06, with the latter dominant solely in the wavelength region $2h$—$3h$, the precise range energized by dispersion error. Viewing Figure 3, the UW and B66 constructions induce artificial diffusion throughout the entire wavenumber spectrum, which will totally compromise the accuracy of the corresponding discrete approximate solution!

Input data error

No theory exists for characterizing human input error in defining an FEA simulation! The large majority of PDEs + BCs + IC statements in continuum mechanics are elliptic boundary value (EBV) for Pa^{-1} finite, hence analytical PDE theory requires BCs be specified on the entirety of the solution domain boundary $\partial\Omega$. For example, CFD simulations require BCs be specified on outflow boundary segments, when in fact the exiting flow state depends on the solution within the domain Ω. Except for pressure, the sole practical outflow BC is vanishing normal derivative, which must be enforced sufficiently remote from major flow activity within Ω to not compromise the interior solution. An example from structural mechanics is the fixed displacement BC. Due to Poisson ratio effects, over-constraining can lead to singular stress concentration behavior, solidly predictable using solution adapted mesh refinement. Another example from CFD is improper wall region meshing when using wall-function BCs for turbulent flow prediction. The theory requires that the resultant solution exhibit a limited range of the $y^+(\mathbf{x},t)$ distribution, a constraint *a priori* unknown until the solution is generated. Again, solution adapted regular mesh refinement will clearly lead to resolution.

DISCUSSION AND RESULTS

Presented herein are data from pertinent computational experiments, conducted using Matlab and COMSOL, illustrating quantification of discrete approximate solution engineering accuracy via error estimation/recognition.

Approximation error

For Pa finite, (7) predicts the asymptotic convergence rate to the accurate solution depends on the FE basis completeness degree k if and only if the data are sufficiently smooth. Consider beam design, Figure 4a), the purpose of which is to control of displacement/stress distributions for anticipated loadings. Simplifying the engineering momentum conservation principle via Euler-Bernoulli beam theory generates; a) a single linear, second-order in time fourth-order in space ($m = 2$) PDE for mechanical vibration, or b) a single fourth order or two second order ($m = 1$) PDEs for steady state loadings. Conversely, steady Timoshenko beam theory generates a pair of second order PDEs, with the caveat that under-integrating the coupling term, which constitutes insertion of numerical diffusion, can improve coarse mesh solution accuracy.

Both steady beam theory GWS^h implementations were tested using Lagrange FE trial space bases $\{N_k(\mathbf{x})\}$, $1 \leq k \leq 3$, also the Hermite $k = 3$ basis with two DOF/node, for a variety of distributed and point loadings. The computed data confirm that for a uniform distributed or isolated point load, all beam theory GWS^h implementations yield solutions converging at the optimal rate $2k$. For the dual ($m = 1$) PDE system Lagrange basis implementation, deflection accuracy of 0.1% was assured via (7) for uniform meshes containing M = 100/30/10 elements for $k = 1/2/3$ bases. The corresponding solution DOF number 201/121/61, hence use of $k > 1$ bases does yield a return on investment. The cubic Hermite basis solution convergence was only $O(h^4)$, not the $O(h^6)$ for the $k = 3$ Lagrange basis, as theoretically predicted in (7) via $2\gamma = 2(k + 1 - m) = 2(3 + 1 - 2) = 4$.

Conversely, changing the problem data slightly to partially distributed with an off-center point load, Figure 4b), all FE degree k basis GWS^h

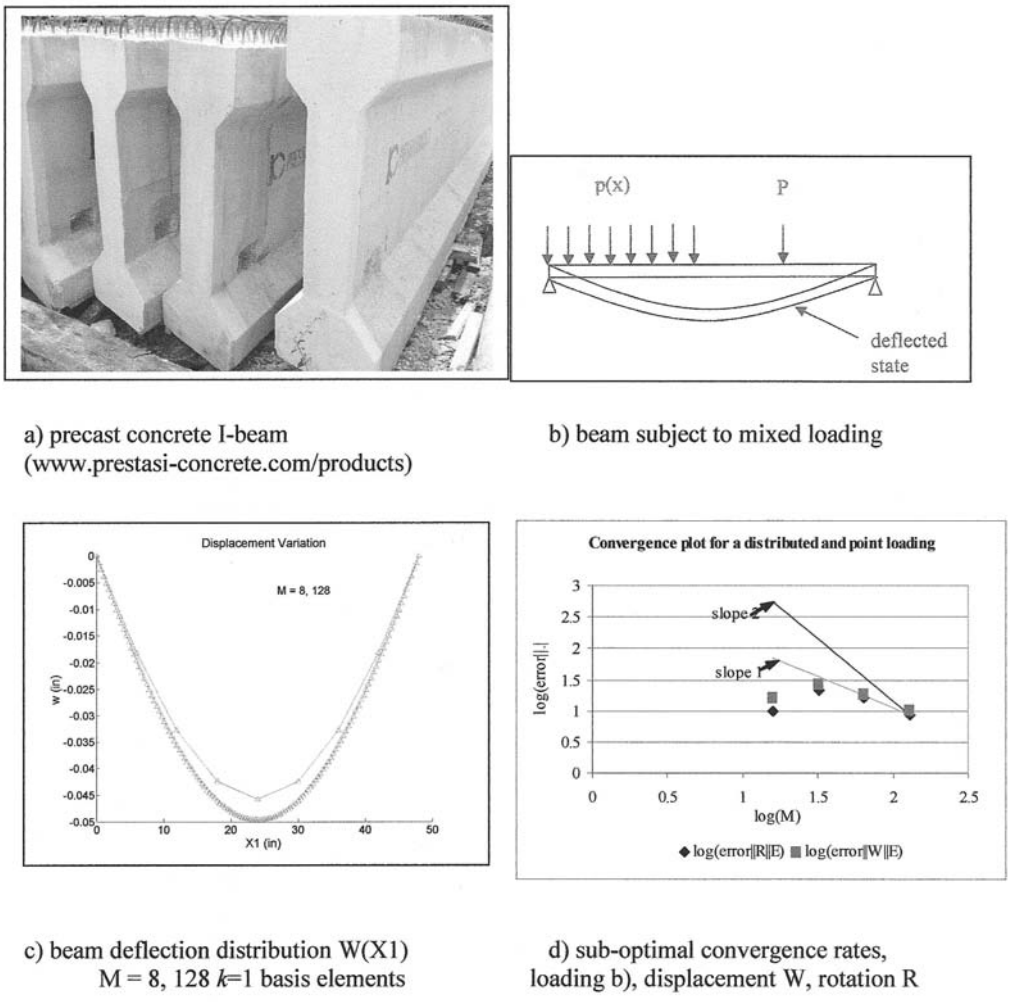

a) precast concrete I-beam (www.prestasi-concrete.com/products)

b) beam subject to mixed loading

c) beam deflection distribution W(X1) M = 8, 128 k=1 basis elements

d) sub-optimal convergence rates, loading b), displacement W, rotation R

Fig. 4. Timoshenko beam theory, illustration of problem statement, GWS^h algorithm solutions for mixed loading with sub-optimal asymptotic convergence, from [25].

implementations for either beam theory produced solutions exhibiting the sub-optimal convergence rate of ~ $O(h^1)$ rather than $O(h^{2k})$! Thereby, as predicted by the theory, the $(r-m)$ term in (7) dominates k due to data non-smoothness of this quite practical load specification (which certainly does not appear very non-smooth!). The resulting mesh requirement for deflection accuracy of 0.1% increases by a factor of nominally four. For the Timoshenko beam theory GWS^h implementation, Figure 4c) graphs the deflection profiles for this loading on M = 8 and M = 128 element meshes. Figure 4d) graphs the associated sub-optimal convergence rates for both DOF, with the off-slope data symbols solidly quantifying under-integration improving coarse mesh accuracy.

In heat transfer, a problem statement seeks the nominal steady state temperature distribution in a motorcycle air cooled engine finned cylinder design, nonlinear due to internal radiation loading with the fins air cooled by convection, Figure 5a). Symmetries admit analysis of the generic cylinder-fin axisymmetric segment, Figure 5b), with the imposed Robin BCs illustrated. For uniform thickness fins GWS^h solution convergence rates are indeed $O(h^{2k})$, even though the solution is but piecewise continuous, Figure 5c). Conversely, for the theoretically predicted optimal fin design of tapered to a point, the solution convergence rates degrade to $O(h^1)$, Figure 5d), for any FE basis degree k implementation. Thus is generated the requirement for a factor of four increase in mesh resolution to generate an engineering accurate solution.

Dispersion error

Dispersion error results from the inability of the mesh supporting the discrete algorithm solution to resolve large wavenumber m spectral content. The COMSOL simulation of convective heat transfer in a cross flow heat exchanger illustrates solution adapted regular mesh refinement assessment and correction. The problem statement and solution process, fully detailed in [25, Ch. 11], is summarized in Figure 6. The top graphic shows the flow geometry with BC periodic symmetry planes which

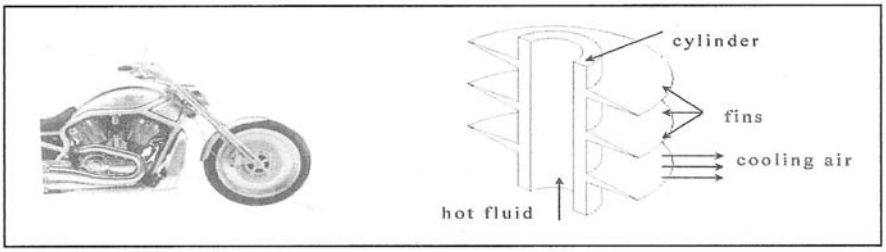

a) motorcycle air cooled engine finned cylinder design

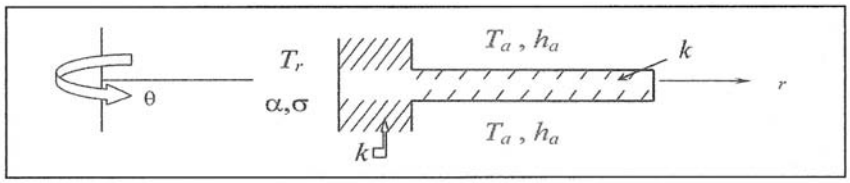

b) generic cylinder-fin segment for analysis with data and BCs

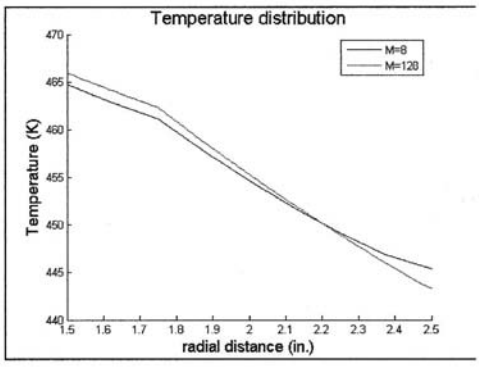

c) piecewise continuous temperature distributions

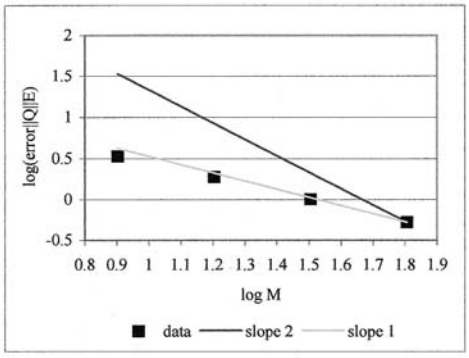

d) tapered fin sub-optimal convergence

Fig. 5. Steady nonlinear heat transfer in a finned cylinder, top & middle: problem specification, left: GWS^h algorithm temperature distributions, right: sub-optimal asymptotic convergence rate for optimal performance tapered fin, from [25].

enables focus on the typical cylinder. The middle graph presents the COMSOL GWS^h temperature distribution with velocity vector overlay for the mildly forced convection case of laminar flow at Re = 250.

The appropriate asymptotic error estimate is (7), and $Pa^{-1} = 0.004$ is small enough to anticipate dispersion error. The bottom graphic compares transverse temperature distributions in the wake immediately downstream of the cylinder. The COMSOL auto-generated M = 1014 triangular element mesh solution is totally polluted by dispersion error, clearly visible as oscillations on the scale of the mesh. Solution adapted regular mesh refinement in the local region produced an M = 4632 element mesh which eliminates the dispersion error everywhere except directly downstream of the cylinder edge, the smoother temperature profile in the graphic. The total elimination of dispersion error in this temperature profile required an M = 15,316 solution adapted mesh, an order of magnitude increase from the auto-generated mesh.

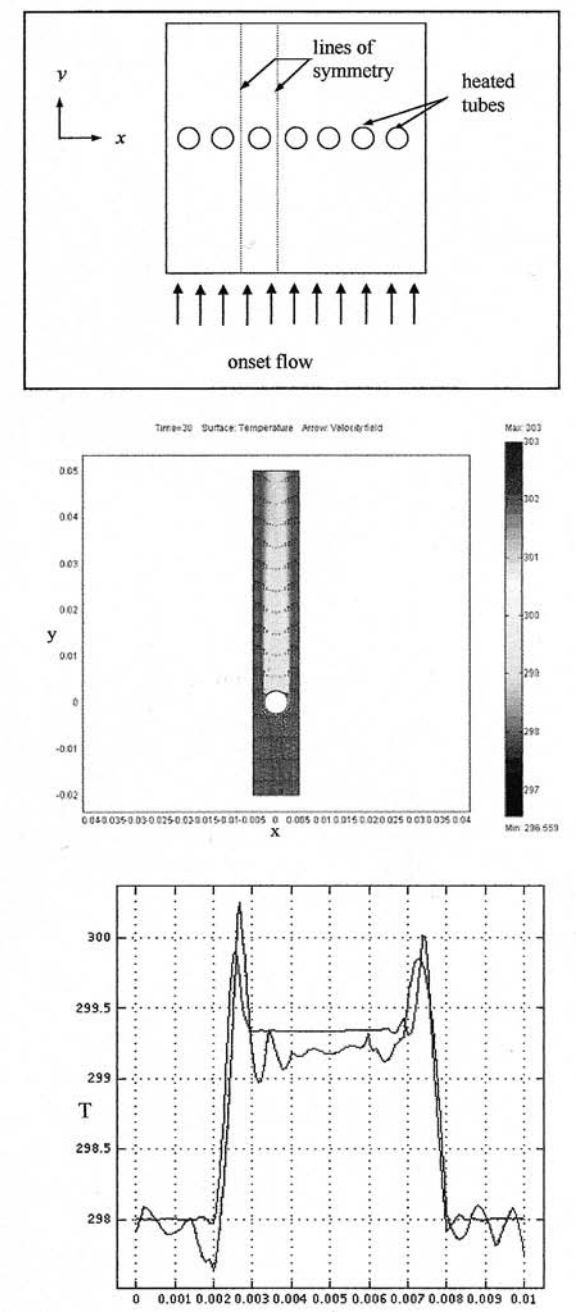

Fig. 6. COMSOL solution-adapted uniform mesh refinement process for steady convective heat transfer in a cross flow heat exchanger, Re = 250, top: problem geometry, middle: steady temperature distribution with velocity overlay, bottom: M = 1014 and solution adapted locally refined M = 4632 temperature profile comparison directly downstream of cylinder, from [25].

In combustion or biological contaminant transport, accurate convection of mass fraction distributions by the velocity field is mandatory. The associated CFD algorithm attribute is phase accuracy, recall Figure 2, and even modest dispersion error can be devastating to prediction fidelity. The premier verification test for quantifying algorithm dispersion error is called the rotating cone, [25, Ch. 11], which defines the planar unsteady convective transport of a gaussian-shaped (smooth and spectrally rich) mass fraction distribution by a rotational velocity field for the limiting specification $Pa^{-1} = 0$. The analytical solution after innumerable complete circular tracks around the solution domain, see Figure 7 inset, is exact preservation of the gaussian IC, shown in perspective in the upper left graph of Figure 7.

Discrete convective transport algorithms generate solution dispersion error to degree dependent on their phase velocity error spectrum, Figure 2. The remaining five graphs in Figure 7 summarize select CFD algorithm theory solutions in the perspective of the IC graph, following the time required to precisely transport the gaussian IC once around the domain in the clockwise direction. The dark shaded contours correspond to solution negative mass fraction, as generated by the phase velocity error spectrum of each algorithm. The Crank-Nicolson FD algorithm, Taylor series second order accurate in space and time, produces the poorest solution, top right graph in Figure 7. The IC 100% peak is decreased by more than 50%, due exclusively to large wavenumber m spectral content cascading to the clearly evident longer wavelength oscillations.

The remaining solutions in Figure 7 are generated by a range of independently theorized GWS^h $k = 1$ basis algorithms. The middle two and lower left solution graph solutions exhibit modest to minimal dispersion error pollution, as evidenced by the darker contour distributions, with an attendant progressive loss in peak level from 96% to 81%. The modified GWS^h algorithm ($\gamma = -0.5$, [27]) solution, lower right, exhibits 100% peak retention while generating the minimal dispersion error magnitude within the class evaluated. The Fourier spectral theory, Figure 2, precisely predicts this relative performance, and additional theoretical material plus computed results on non-carte-

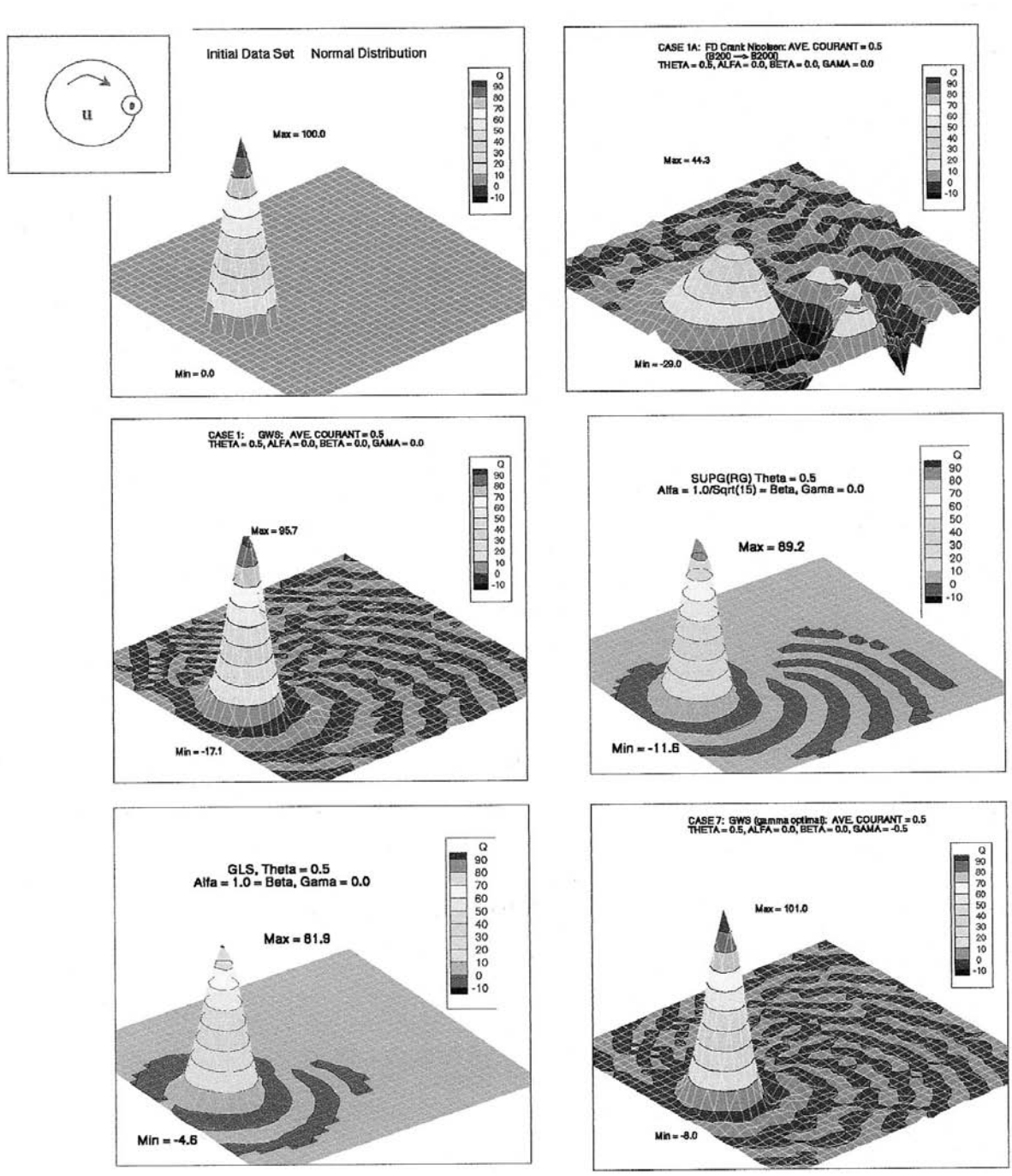

Fig. 7. Rotating cone mass transport verification problem, select algorithm solutions after one revolution, uniform Cartesian M = 32 × 32 quadrilateral mesh, trapezoidal time algorithm, Courant number $|\mathbf{C}|$ = 0.3 at IC centroid, from [27].

top left: IC, exact solution, with problem essence in inset
top right: Crank-Nicolson FD algorithm
middle left: $k = 1$ basis base GWS^h algorithm
middle right: $k = 1$ basis Petrov-Galerkin GWS^h algorithm
bottom left: $k = 1$ basis Least Squares GWS^h algorithm
bottom right: $k = 1$ basis, optimal $\gamma = -0.5$ GWS^h algorithm

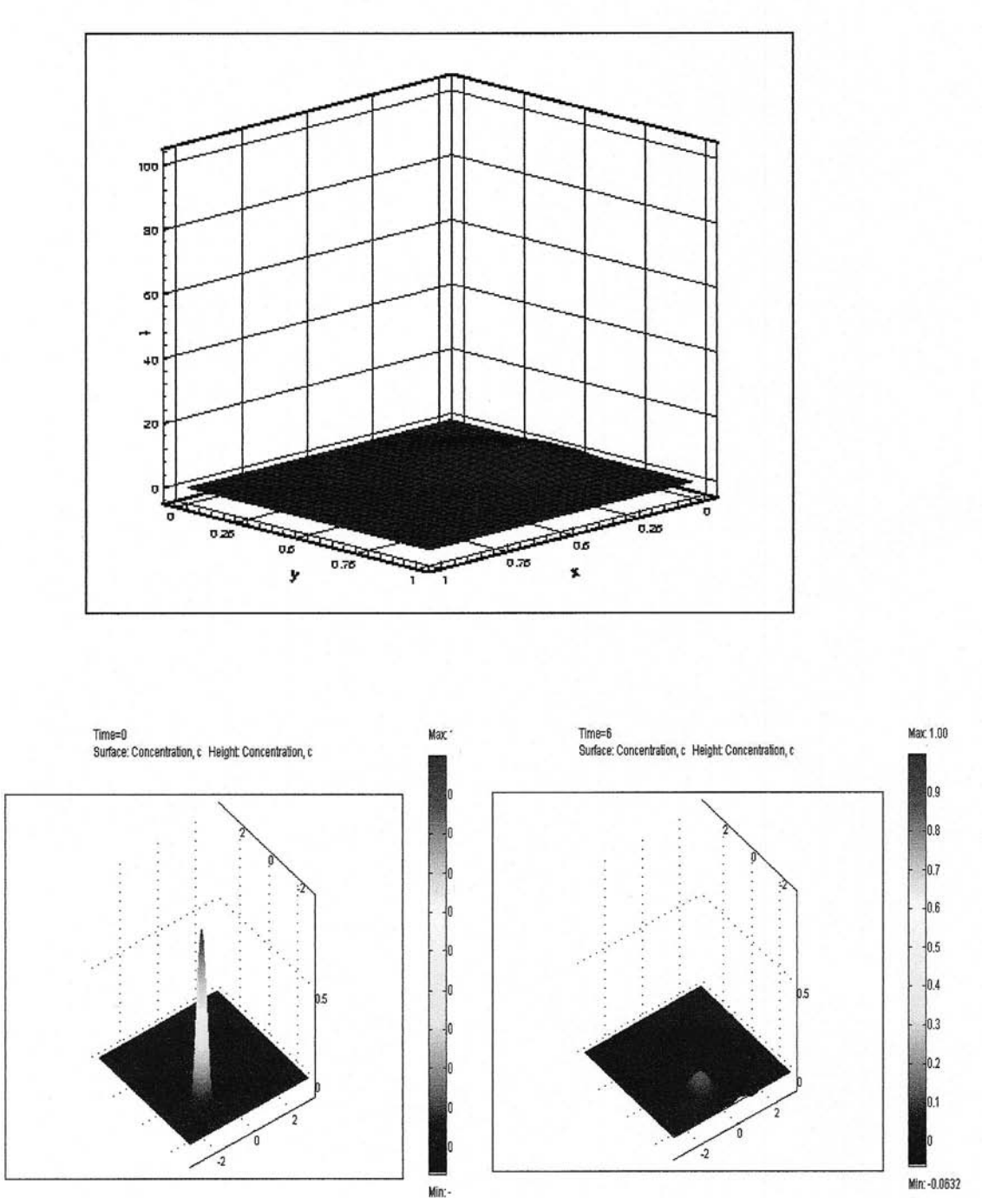

Fig. 8. Rotating cone mass transport verification problem, select dissipative algorithm solutions after one revolution, uniform Cartesian M = 32 × 32 quadrilateral mesh, trapezoidal time algorithm, Courant number $|\mathbf{C}| = 0.3$ at IC centroid, from [27].

top: Crank-Nicolson upwind FD algorithm "vanished" solution
left: $k = 1$ basis COMSOL GWS^h algorithm IC (for reference)
right: $k = 1$ basis COMSOL anisotropic diffusion and SUPG GWS^h solutions

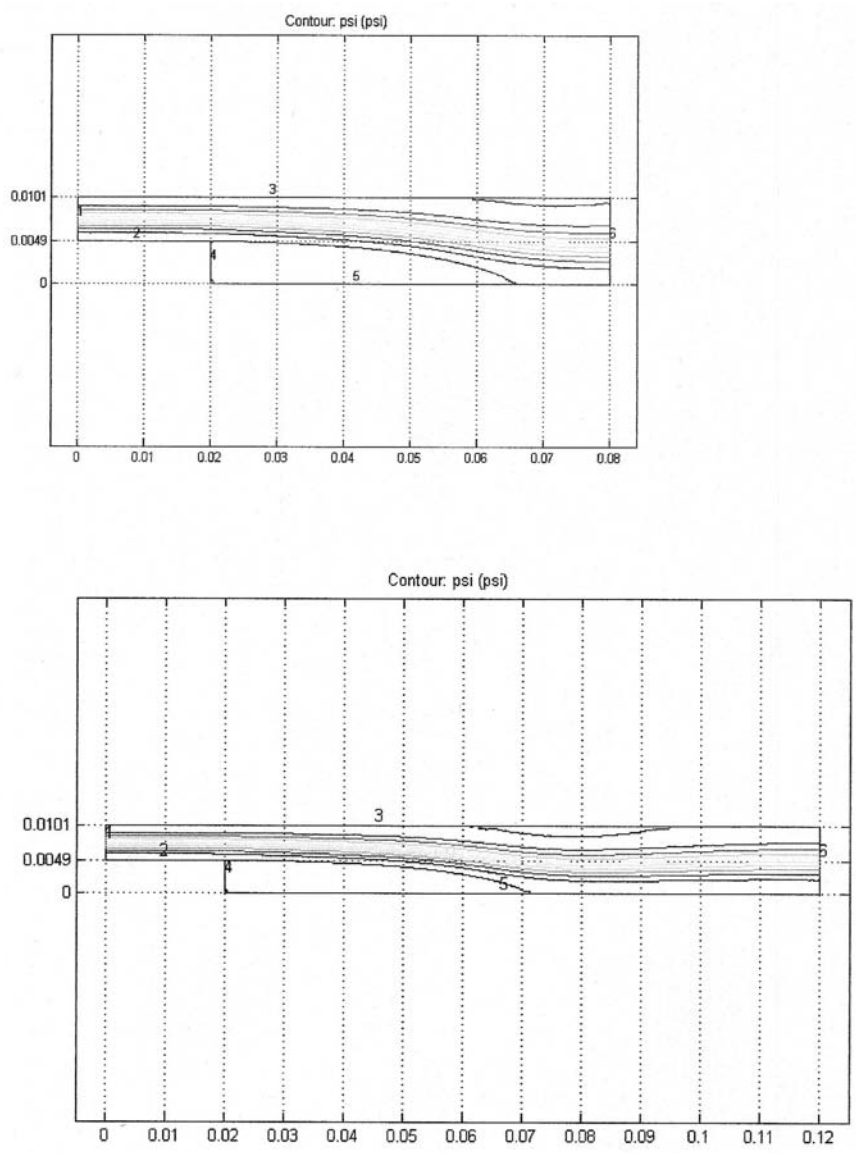

Fig. 9. Steady flow stepwall diffuser problem, COMSOL vorticity-streamfunction GWS^h algorithm, Re = 600 solutions, top: streamlines on M = 2573 element mesh, bottom: streamlines on extended M = 3807 element mesh, from [25].

sian meshes, which further aggravates dispersion error generation hence solution inaccuracy, is available, [27].

Numerical diffusion error

Dispersion error thoroughly complicates solution processes for transport problem simulations at small Pa^{-1}. In practice, only for simulations with $Pa^{-1} \geq O(10^{-3})$ is a stable algebraic process possible without embedding artificial diffusion. The COMSOL crossflow heat exchanger example at Re = 250 ($Pa^{-1} = 0.004$), Figure 6, well illustrates this point, but real world simulations have Re two orders of magnitude larger than 250! Hence, the use of numerical diffusion is mandatory to generate stable algebraic processes for multi-physics simulations at realistic Pa^{-1} which creates the genuine vs. artificial *physics* assessment requirement.

The Fourier modal theory characterization of numerical diffusion is established, recall Figure 3. The rotating cone verification problem provides clear assessment of discrete solutions polluted by numerical diffusion. The Crank-Nicolson upwind (UW in Figures 2–3) is an $O(h^1)$ dissipative algorithm. Recalling the exact solution in Figure 7 upper left, repeating the single translation simulation using the UW algorithm generates the solution graph at the top of Figure 8. It is indeed dispersion error-free but is totally diffused to a null peak magnitude, a completely erroneous solution!

FEA transport options in COMSOL include the streamline-upwind Petrov-Galerkin (SUPG) and anisotropic diffusion GWS^h algorithms, both of which via theory are $O(h^2)$ dissipative, [27]. The gaussian IC via COMSOL-generated graphics is shown at bottom left of Figure 8, with the single circular translation solution using either algorithm

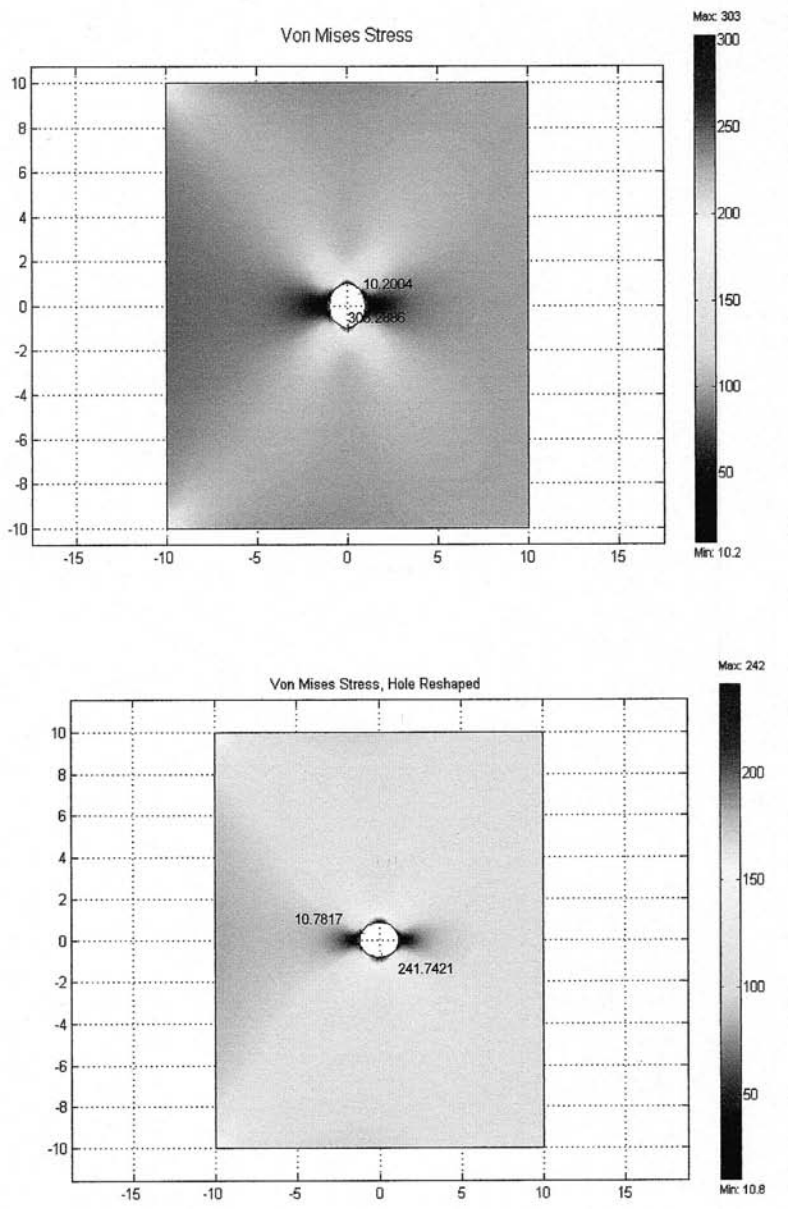

Fig. 10. Plane stress elasticity, plate in tension with hole von Mises stress distributions, COMSOL GWS^h algorithm, top: original circular hole, M = 1068 element mesh, bottom: optimal elliptical hole, M = 4272 element mesh, from [25].

graphed at bottom right. Both algorithms solutions are devoid of dispersion error and both are absolute garbage due to the imposed numerical diffusion level.

Bottom line: the simulation specialist must be cognizant that improper use of artificial diffusion will produce smooth solutions that are totally engineering inaccurate! The solution adaptive mesh refinement process is mandatory to sort out genuine versus artificial physics issues for transport simulations.

Input data error

As stated, most multi-physics PDEs + BCs + IC statements are elliptic boundary value for $Pa^{-1} > 0$, hence BCs must be specified on the domain boundary $\partial\Omega$ entirety. In CFD, the admissable outflow BC is vanishing normal derivative, and this boundary segment must be appropriately distant. A COMSOL CFD validation exercise (since it possesses comparative experimental data) clearly illustrates solution corruption by the outflow BC too close to a step wall diffuser. Solutions are parameterized by Pa = Re, the step-induced recirculation region extent grows with Re, and for Re > 400 a top surface secondary recirculation region is generated which intersects the outflow BC, Figure 9 top. The correction is to extend the solution domain, Figure 9 bottom, which eliminates the 10% error in reattachment coordinate predicted using the too-short domain.

In plane elasticity, a COMSOL exercise requires

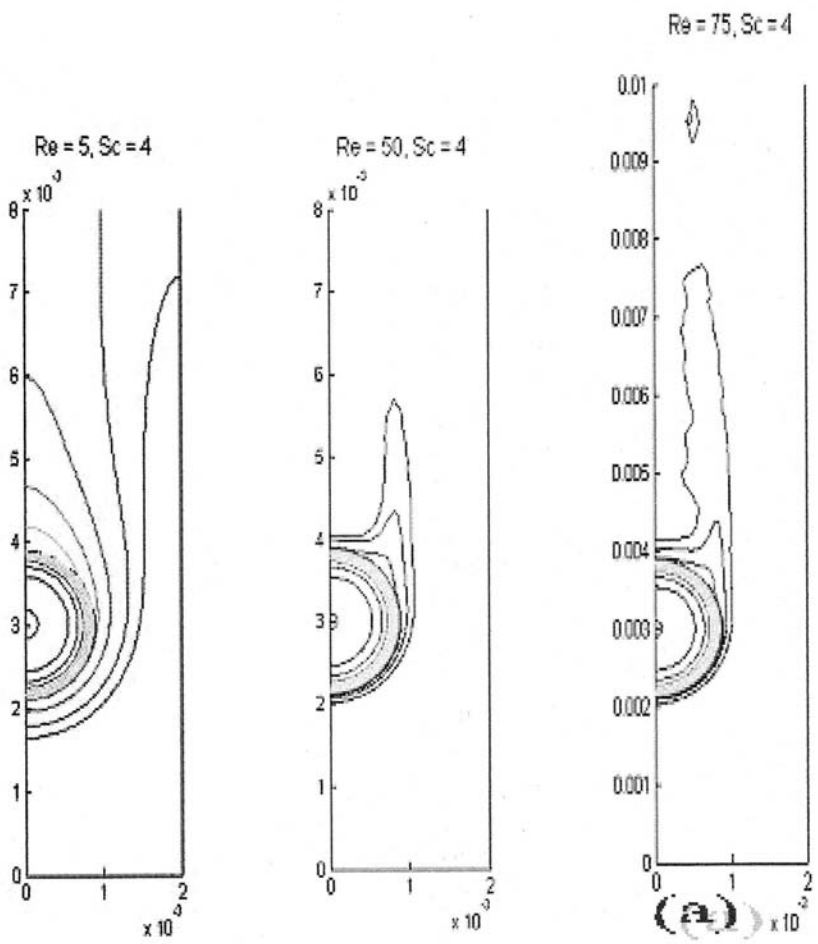

Fig. 11. Mass transfer from a catalyst pellet in creeping cross flow, COMSOL GWS^h algorithm, Sc = 4: left to right, Re = 5, 25, 75 steady state GWS^h solutions, from [25].

altering an initially circular hole in a plate, assumed rigidly attached to a wall and subject to tension, to minimize the von Mises stress concentration, Figure 10 top. The corresponding wall displacement vector BC is zero. Altering the hole to any geometry with "corners," e.g., triangle, square, and running the COMSOL-automated mesh solution process generates a von Mises stress concentration lower than the original circular hole, which of course is totally fallacious. Conducting solution adaptive regular mesh refinement about any such shape correctly generates a divergent solution.

The correct circle alteration is to an ellipse with major axis parallel to the applied load. As the major/minor axes are scaled with COMSOL-automated mesh refinement, the extremum stress concentration moves to the plate corners where the rigid BC is applied. Again, solution adaptive regular mesh refinement will correctly predict this rigid BC is inappropriate, but the COMSOL-automated mesh refinement process does not catch it. The resultant conclusion is that only the load-parallel displacement can have a rigid BC, whence the optimal hole shape is confirmed the ellipse leading to a 30 ksi reduction in von Mises stress extremum, Figure 10 bottom.

A BC specification-intense multi-physics COMSOL simulation is for mass transfer from a catalyst pellet array into a creeping (small Re) cross flow stream. The simulation requires coupling of the incompressible Navier-Stokes (NS) with the chemical engineering convection-diffusion module (with its harmonic PDE). The pertinent non-D groups are Reynolds and Schmidt number, Re, Sc, and all PDEs are EBV statements. The pellet-fluid interface BCs are no slip and continuous mass fraction (distribution), while symmetry plane BCs bisect the pellet and the pellet separation distance. At outflow the NS BC is vanishing normal derivative with fixed pressure, while the harmonic PDE requires a local, solution-dependent operation corresponding to vanishing normal derivative.

Figure 11 graphs the COMSOL-computed steady mass fraction distributions for Sc = 4 and $5 \leq \text{Re} \leq 75$. The mass diffused into the flow field progressively coalesces into a plume with increasing Re, indicating transition from diffusion to convection domination. The oscillations in the Re

= 75 solution mass fraction contour plot are clear evidence of dispersion error pollution, also inappropriate downstream BC location, even though the solution domain downstream extent was increased. These critical data observations confirm the COMSOL-automated M = 2147 refined mesh supporting this solution is inadequate and must be altered via solution adapted regular refinement to generate an *engineering accurate solution*!

SUMMARY AND CONCLUSIONS

Modern problem solving environments, specifically COMSOL, readily support multi-physics simulations of engineered systems design performance. Genuine applications invariably couple conservation principles across the spectrum of engineering continuum mechanics, i.e., structures, vibrations, fluid dynamics, heat/mass transport, acoustics, electromagnetics. The resultant *new* academic engineering discipline is the computational engineering sciences, and PSEs like COMSOL transform these math-physics descriptions to computable form via finite element analysis (FEA) methodology. The associated theoretical underpinnings have been thoroughly developed and illustrated via insightful computational exercises, many performed using COMSOL.

The informed use of a PSE can indeed provide engineering accurate data impacting design optimization. Assuring a quality prediction requires the analyst possess dexterity with the fundamental theory underlying FEA, in particular be cognizant of the error mechanisms inherent in this approximation procedure. This article has introduced the four basic categories of FEA error mechanism, and provided brief but substantive guidance on quantitative assessment protocols via insightful examples. The fundamental requirement is to employ *solution adaptive regular mesh refinement* to generate a sequence of data sets that, using the available theory, can quantify that error mechanisms do not dominate.

In conclusion, options exist for the professional engineer using COMSOL in commercial practice to be exposed to the full academic content that underlies this article. These may be viewed by touching Collaboratory in the left hot word column at the CFD Lab home page cfdlab.utk.edu Self-paced professional self-study options also exist totally independent of the Internet modality, www.jcomputek.com

Acknowledgments—The majority of the academic material supporting this technical content was completed during the graduate student tenure of the three coauthors. Aspects of this research were supported by the US National Science Foundation (NSF), Award Number 0121669, which is gratefully acknowledged. The lead author has enjoyed a long term collegial association with select technical principals of COMSOL.

REFERENCES

1. A. Hrenikoff, Solution of Problems in Elasticity by the Frame Work Method. *J. Applied Mechanics, ASME Transactions*, **8**, (1941), pp. 169–175.
2. R. Courant, (1943), Variational Methods for Solution of Problems of Equilibrium and Vibrations. *Bull. Amer. Math. Soc.*, **49**, (1943), pp. 1–23.
3. M. Turner, R.W. Clough, H. Martin and L. Topp, Stiffness and Deflection Analysis of Complex Structures. *J. Aeronautical Sciences,* **23**(9), (1956), pp. 805–823.
4. R. W. Clough, (1960), The Finite Element Method in Plane Stress Analysis. *Proc. 2nd ASCE Conf. Electronic Computation*, (1960), pp. 345–378.
5. J. H. Argyris, *Recent Advances in Matrix Methods of Structural Analysis*. Pergamon Press, Elmsford, NY (1963).
6. O. C. Zienkiewicz and Y. K. Cheung, Finite Elements in the Solution of Field Problems. *The Engineer*, (1965), pp. 507–510.
7. J. W. S. Raleigh, *Theory of Sound*, 1st Ed. Revised (1945), Dover, New York (1877).
8. W. Ritz, Uber Eine Neue Methode zur Losung Gewisser Variations-Probleme der Mathematishen Physik. *J. Reine Angew. Math*., **135**, (1909), pp. 1.
9. B. A. Finlayson, *The Method of Weighted Residuals and Variational Principles*. Academic Press, New York (1972).
10. B. G. Galerkin, Series Occurring in Some Problems of Elastic Stability of Rods and Plates, *Engineering Bulletin,* **19**, (1915), pp. 897–908.
11. J. T. Oden, Finite Element Applications in Fluid Dynamics. ASCE, *J. Engineering Mechanics Div.*, **95**, EM3, (1969), pp. 821–826.
12. J. T. Oden, *Finite Elements of Nonlinear Continua*. McGraw-Hill, New York (1972).
13. A. J. Baker, Finite Element Solution Algorithm for Viscous Incompressible Fluid Dynamics. *J. Numerical Methods Engineering*, **6**, (1973), pp. 89–101.
14. A. J. Baker, A Finite Element Algorithm for the Navier-Stokes Equations. NASA Technical Report CR-2391 (1974).
15. M. E. Olsen, Formulation of a Variational Principle-Finite Element Method for Viscous Flows, *Proc. Variational Methods Engineering,* Southampton University, UK, 5.27-5.38 (1972).
16. P. O. Lynn, Least Squares Finite Element Analysis of Laminar Boundary Layers. *J. Numerical Methods Engineering*, **8**, (1974), pp. 865–878.
17. J. T. Oden and J. N. Reddy, *An Introduction to the Mathematical Theory of Finite Elements*. Wiley-Interscience, New York (1976).
18. Z. Popinski and A.J. Baker, An Implicit Finite Element Algorithm for the Boundary Layer Equations, *J. Computational Physics*, **21**, (1976), pp. 55–84.

19. M. O Soliman and A. J. Baker, Accuracy and Convergence of a Finite Element Algorithm for Laminar Boundary Layer Flow, *J. Computers and Fluids*, **9**, (1981), pp. 43–62.
20. M. O. Soliman and A. J. Baker, Accuracy and Convergence of a Finite Element Algorithm for Turbulent Boundary Layer Flow. *Computer Methods Applied Mechanics & Engineering*, **28**, (1981), pp. 81–102.
21. J. J. Conner and C.A. Brebbia, *Finite Element Techniques for Fluid Flow.* Newnes-Butterworths Publishers, UK (1974).
22. G. F. Pinder and W. G. Gray, *Finite Element Simulation in Surface and Subsurface Hydrology.* Academic Press, New York (1977).
23. A. J. Baker, *Finite Element Computational Fluid Mechanics*. Hemisphere/McGraw-Hill, New York (1983).
24. J. T. Oden and L. F. Demkowicz, *Applied Functional Analysis*, CRC Press, Boca Raton, FL (1996).
25. A. J. Baker, *The Computational Engineering Sciences*. j-Computek Press, Loudon TN (2006).
26. I. Babuska and W.C. Rheinboldt, *a-posteriori* Error Estimates for the Finite Element Method, *J. Numerical Methods Engineering,* **12**, 1976.
27. S. Sahu and A. J. Baker, A Modified Conservation Principles Theory Leading to an Optimal Galerkin CFD Algorithm. *J. Numerical Methods Fluids*, **55**, (2007), pp. 737–783.
28. D. J. Chaffin and A. J. Baker, On Taylor Weak Statement Finite Element Methods for Computational Fluid Dynamics. *J. Numerical Methods Fluids*, **21**, (1997), pp. 273–294.

A. J. Baker is Professor, Engineering Science and Director, CFD Laboratory, at the University of Tennessee (UT), Knoxville TN USA. Joining UT from commercial aerospace in 1975, his research expertise is the computational engineering sciences with a focus in CFD and weak form methods. He has served as major professor for 16 PhD dissertations, advisor for 17 MS theses/projects, and has authored over 280 technical publications in the field. He has written three texts, two with international editions and one Japanese translation, on the computational engineering sciences and CFD. The fourth text, *Optimal Continuous Galerkin Weak Form CFD,* now in draft, will coalesce recent research accomplishments on the subject. He has served as principal investigator/technical director for ~$7 million in CFD and computational sciences research contracts, is an elected Fellow of the US and the International Association for Computational Mechanics and serves on the Editorial Boards of four archival journals.

Sunil Sahu is currently Senior Engineer, Fuel Systems Simulation and Analysis, Large Power Systems, Caterpillar Corporation, Mossville, IL USA. He received his BS in Mechanical Engineering in India in 2000, the MSc in Mechanical Engineering from Tennessee Technological University (TTU), Cookeville, TN in 2002, and the PhD in Mechanical Engineering in 2006. His dissertation was entitled, *A Theory for Modified Conservation Principles Optimization of CFD Algorithm Fidelity*.

Marcel A. Grubert is currently Research Engineer, Advanced Well Simulation Section, Exxon/Mobil Upstream Research Company, Houston, TX, USA. He earned the Diplom Ingenieur (M.Sc. equivalent) in aerospace engineering at the Technical University of Aachen (RWTH), Germany, 1998, and completed the Ph.D. in Mechanical Engineering in 2006 at UT. His dissertation was entitled, *A Potentially Accurate and Efficient LES CFD Algorithm to Predict Heat and Mass Transport in Inhabited Spaces*.

Shawn C. Ericson is currently Senior Engineer, CFD Research Corporation, Huntsville, AL USA. He earned the BS in Mechanical Engineering in 1993 from Tennessee Technological University (TTU), Cookeville, TN USA. After working in the generator and aerospace industries, he completed the M.Sc. in Engineering Science in 2001 specializing in CFD. He subsequently worked on numerous computational engineering science projects at UT, Oak Ridge National Laboratory (ORNL), and the Genome Science and Technology UT/ORNL partnership.